Probiotics and Antimicrobial Proteins (2024) 16:1270–1287
https://doi.org/10.1007/s12602-023-10112-3

RESEARCH

Structural and Biochemical Characterization of Three Antimicrobial Peptides from *Capsicum annuum* L. var. *annuum* Leaves for Anti-*Candida* Use

Milena Bellei Cherene[1] · Gabriel Bonan Taveira[1] · Fabricio Almeida-Silva[2] · Marciele Souza da Silva[1] · Marco Calvinho Cavaco[3] · André Teixeira da Silva-Ferreira[4] · Jonas Enrique Aguilar Perales[4] · André de Oliveira Carvalho[1] · Thiago Motta Venâncio[2] · Olney Vieira da Motta[5] · Rosana Rodrigues[6] · Miguel Augusto Rico Botas Castanho[3] · Valdirene Moreira Gomes[1]

Accepted: 14 June 2023 / Published online: 26 June 2023

Abstract
The emergence of resistant microorganisms has reduced the effectiveness of currently available antimicrobials, necessitating the development of new strategies. Plant antimicrobial peptides (AMPs) are promising candidates for novel drug development. In this study, we aimed to isolate, characterize, and evaluate the antimicrobial activities of AMPs isolated from *Capsicum annuum*. The antifungal potential was tested against *Candida* species. Three AMPs from *C. annuum* leaves were isolated and characterized: a protease inhibitor, a defensin-like protein, and a lipid transporter protein, respectively named *Ca*CPin-II, *Ca*CDef-like, and *Ca*CLTP2. All three peptides had a molecular mass between 3.5 and 6.5 kDa and caused morphological and physiological changes in four different species of the genus *Candida*, such as pseudohyphae formation, cell swelling and agglutination, growth inhibition, reduced cell viability, oxidative stress, membrane permeabilization, and metacaspase activation. Except for *Ca*CPin-II, the peptides showed low or no hemolytic activity at the concentrations used in the yeast assays. *Ca*CPin-II inhibited α-amylase activity. Together, these results suggest that these peptides have the potential as antimicrobial agents against species of the genus *Candida* and can serve as scaffolds for the development of synthetic peptides for this purpose.

Keywords Antifungal · Bioactive peptides · *Candida* genus · *Capsicum annuum*

Introduction

Antimicrobial peptides (AMPs) play a role in the defense and can be expressed constitutively as part of the organism's normal developmental program or induced upon exposure to a stress factor. AMPs contain 12–100 amino acid residues and vary in their conformation and sequence [1, 2]. Many structural classes of AMPs are involved in plant defense, mainly represented by groups of defensins, thionins, lipid transport proteins (LTPs), and circular

✉ Valdirene Moreira Gomes
valmg@uenf.br

[1] Laboratório de Fisiologia e Bioquímica de Microrganismos, Centro de Biociências e Biotecnologia, Universidade Estadual do Norte Fluminense Darcy Ribeiro, Campos dos Goytacazes, RJ 28013-602, Brazil

[2] Laboratório de Química e Função de Proteínas e Peptídeos, Centro de Biociências e Biotecnologia, Universidade Estadual do Norte Fluminense Darcy Ribeiro, Campos dos Goytacazes, RJ 28013-602, Brazil

[3] Instituto de Medicina Molecular João Lobo Antunes, Faculdade de Medicina da Universidade de Lisboa, Lisbon, Portugal

[4] Laboratório de Toxinologia, Instituto Oswaldo Cruz, FIOCRUZ, Rio de Janeiro, RJ, Brazil

[5] Laboratório de Sanidade Animal, Centro de Ciências e Tecnologias Agropecuárias, Universidade Estadual do Norte Fluminense Darcy Ribeiro, Campos dos Goytacazes, RJ 28013-602, Brazil

[6] Laboratório de Melhoramento e Genética Vegetal, Centro de Ciências e Tecnologias Agropecuárias, Universidade Estadual do Norte Fluminense Darcy Ribeiro, Campos dos Goytacazes, RJ 28013-602, Brazil

peptides (i.e., cyclotides) [3, 4]. Structural diversity is the most striking feature of plant AMPs; however, they share some common characteristics such as a relatively low molecular weight (less than 10 kDa) and a variable number of cysteine residues that form disulfide bonds and contribute to the stabilization of the tertiary structure. Different structural classes of AMPs have compact structures and are resistant to chemical and proteolytic degradation. They also have amphipathic properties, with both a positively charged hydrophilic region capable of interacting with anionic residues and a hydrophobic region that interacts with lipids [5, 6]. In general, AMPs have broad inhibitory activity against the growth and development of other organisms such as filamentous fungi, yeasts, bacteria, viruses, protozoa, and insects [1]. AMPs can disrupt and permeabilize membranes by interacting with cell membrane components and/or intracellular targets, inhibiting DNA/RNA and protein synthesis, and controlling or interrupting the growth of microorganisms [7, 8].

The indiscriminate use of antimicrobials has resulted in the emergence of microorganisms that are resistant to conventional drugs. Although often overlooked, pathogenic fungi pose a threat to public health, biodiversity, and food safety [9]. More than 300 million people suffer from serious fungal diseases with an estimated annual mortality of 1.6 million [10]. Almost 4 million people in Brazil are expected to have fungal infections each year. Of this total, 2.8 million are infections caused by *Candida* sp. and 1 million by *Aspergillus* sp., which mainly affect immunocompromised individuals [11]. *Candida* sp. can cause mucosal, cutaneous, and systemic infections, and resistant *Candida* infections are classified as serious by the Center for Disease Control and Prevention (CDC) [12]. Approximately 7% of candidemia cases are resistant to available antimicrobials, and the lethality in hospitalized patients is estimated at 25%. *Candida albicans* is the most prevalent species in candidemia, although it has low resistance levels. Conversely, other species, such as *Candida glabrata* and *Candida parapsilosis* are often resistant and lethal [12, 13].

Because AMPs have diverse mechanisms of action, broad-spectrum activity, and biochemical characteristics that hinder the evolution of resistance, the development of new drugs derived from them is a promising strategy [14, 15]. Additionally, AMPs have the advantage of low or no toxicity to animal cells [16, 17]. In recent years, the genus *Capsicum* has been regarded as an important source of molecules that stand out as possible candidates to overcome microbial resistance to conventional drugs [18]. Several *Capsicum* AMPs have been isolated and characterized, including defensins [19–21], lipid transport proteins (LTPs) [22], proteinase inhibitors [22–24], thionin-like peptides [25], ɣ-thionins [26], and hevein-like peptides [27]. The mechanisms of action of the AMPs isolated from *Capsicum* have not been completely elucidated; however, they have been shown to trigger events that activate programmed cell death [28], including morphological changes, increased membrane permeabilization, production of reactive oxygen species (ROS), and dissipation of mitochondrial potential [24, 25, 29]. In previous work, our research group purified and characterized several AMPs isolated from *C. annuum*. Here, we isolated, characterized, and evaluated the antifungal activity and mechanisms of action of three AMPs isolated from *C. annuum* leaves.

Materials and Methods

Biological Material

Seeds of *Capsicum annuum* L. var. *annuum* (cv. Carioquinha) were provided by the Laboratório de Melhoramento Genético Vegetal, Centro de Ciências e Tecnologias Agropecuárias, Universidade Estadual do Norte Fluminense Darcy Ribeiro, (UENF), Campos dos Goytacazes, Rio de Janeiro, Brazil. Seeding was carried out in polyestirene foam of 72 cells with commercial substrate and kept in a growth chamber with a controlled temperature of 28 °C and a photoperiod of 12 h. When the seedlings exceeded 10 cm in height, they were transplanted into 5 L pots and transferred to the greenhouse. At 60 days, the leaves were cut close to the petiole and used for peptide extraction.

The yeasts *Candida tropicalis* (CE017), *Candida albicans* (CE022), and *Candida parapsilosis* (CE002) were provided from Departamento de Biologia, Universidade Federal do Ceará, Fortaleza, Brazil. The yeast *Candida buinensis* (3982) was provided from Micoteca URM from Universidade Federal de Pernambuco, Recife, Pernambuco, Brazil. *Candida* yeasts were kept on Sabouraud 2% glucose agar (Merck) at the Laboratório de Fisiologia e Bioquímica de Microrganismos, from Centro de Biociência e Biotecnologia, UENF, Campos dos Goytacazes, Rio de Janeiro, Brazil.

Extraction, Purification, and Biochemical Characterization of Peptides

C. annuum leaves (10 g) were macerated and extracted with 30 mL of 60% methanol (v/v) at room temperature over a period of 24 h. The extract was filtered to remove debris and partitioned with dichloromethane (1:1, v/v) at room temperature for a period of 24 h and the aqueous phase were separated and concentrated by lyophilization.

The leaves extract (0.1 g) was dissolved in 10 mL of 20% acetonitrile, filtered with 0.22 µm pore size Millex® syringe

filter and injected onto a high-performance liquid chromatography (HPLC) VP-ODS (250 × 4.6 mm i.d.) C_{18} reverse-phase column (Shim-pack, Shimadzu) with a C_8 guard column (*Pelliguard*, Sigma). The column was equilibrated with 10 mL of solution A (0.1% trifluoroacetic acid (TFA)), and eluted with 100% solution A for the first 2 min followed by a gradient of solution B (90% acetonitrile containing 0.1% TFA). The concentration of solution B was maintained at 0% for 2 min; increased to 10% from 2 to 10 min; to 50% from 10 to 102 min and maintained at 50% for 1 min. Then, the concentration of solution B was reduced to 0% and was kept at 0% until the end of the run at 110 min. The chromatography was developed at a flow rate of 0.5 mL min^{-1} at a temperature of 37 °C. The presence of proteins was determined by online absorbance measurement at 220 and 280 nm.

Proteins quantifications were done by the bicinchoninic acid (BCA) method described by Smith et al. [30], with modifications, using ovalbumin as the protein standard. SDS-tricine-gel electrophoresis was performed according to the method described by Schagger and von Jagow [31].

Amino acid sequence analysis was done using time of flight mass spectrometry (MALDI-TOF) on peptides isolated from HPLC fractions P_0, P_1, and P_2. The fractions were subjected to SDS-tricine-gel electrophoresis and the single band from each fraction was excised from the gel, digested with trypsin, and subjected to a mass spectrometry evaluation. Tryptic peptide fragments were analyzed by matrix-assisted laser desorption ionization time-of-flight mass spectrometry (MALDI-TOF MS). The instrument used was Orbitrap Q Exactive Plus (Thermo Scientific). Sequence similarity searches were performed using BLASTp and the nonredundant protein database (nr) [32] for P_1 and P_2, while P_0 was analyzed using the PINIR (Pin-II type PIs Information Resources) database [33]. Selected sequences were aligned with ClustalW [34].

Circular dichroism (CD) spectra of the three peptides were acquired in a J-815 CD spectropolarimeter (Jasco, Japan) at 25 °C in the 190–260 nm wavelength range, with a bandwidth of 0.50 nm and a scan speed of 50 nm/min, using a 0.1 cm quartz cell. Further, 200–400 µg mL^{-1} peptide solutions were prepared in ultra-pure water. The final spectra for each peptide were the average of ten consecutive scans per sample after subtraction of buffer baselines. Results were expressed as mean residue ellipticity ($[\theta]_{MRW}$) (deg × cm^2 × $dmol^{-1}$), as follows:

$$\mathrm{MRW} = \frac{\theta_{oBS} \times \mathrm{MRW}}{10 \times d \times c} \quad (1)$$

where Θ_{obs} is the observed ellipticity in degrees, MRW is the mean residue weight, d is the cell path length, and c is the peptide concentration.

The peptide fragments were searched against the nonredundant protein sequence database using BLASTp [32], revealing XP_016579689.1 and KAF3615994.1 as best hits (defensin and non-specific LTP 2, respectively) and the sequence P56615 (UniProt ID) with 100% similarity with *C. annuum* protease inhibitor. These sequences were searched against the AlphaFold DB [35] using the EBI Protein Similarity Search tool (https://www.ebi.ac.uk/Tools/sss/fasta/). The AlphaFold model of the best orthologs (Q9FFP8 for defensin and A0A0R0FHG0 for nsLTP2) and P56615 (for protease inhibitor) were used as templates for homology modeling with Phyre2 [36] using one-to-one threading mode. Modeling of the 35 amino acid residue fragment RLCTNCCAGRKGCNYYSADGTFICEGESDPNNPKA found in the mass spectrometry analysis of peptide P_0 (*Ca*CPin-II) was done with Phyre2.

In Silico Prediction of Cell-Penetrating Potential

For increased confidence, we used three independent machine learning-based approaches that use random forest classifiers to predict the cell-penetrating potential of peptides: SkipCPP-Pred [37], MLCPP [38], and CellPPD-Mod [39]. Results obtained from SkipCPP-Pred analyses have confidence scores ranging between 0 and 1 (1 is the maximum confidence). MLCPP probability scores is the probability of permeabilizing membranes, which ranges from 0 to 1 (1 is the greatest ability to permeabilize). Additionally, we performed a BLAST search for similar cell-penetrating peptides in the CPPsite 2.0 database [40] using P56615, XP_016579689.1 and KAF3615994.1 as queries. Predictions of cell-penetrating potential of the defensin were performed under three scenarios: mature peptide sequence, γ-core, and γ-core plus two upstream and downstream residues, based on antimicrobial activity evidence from a previous work [41].

Effect of Peptides on Yeast Growth

An inoculum from each *Candida* stock was transferred to Petri dishes containing Sabouraud agar and incubated at 30 °C for 24 h. After this period, the yeast cells were transferred to a liquid culture medium Sabouraud dextrose broth (10 mL). Yeast cells were count in a Neubauer chamber (Optik Labor) for further calculation of appropriate dilutions. A yeast growth inhibition quantitative assay was performed following the method described by Broekaert et al. [42], with some modifications. Yeast cells (1×10^4 cells mL^{-1}) were treated with peptides at increasing concentrations from 1.56 to 200 µg mL^{-1} diluted in 100 µL of Sabouraud dextrose broth. The assay was performed on cell culture microplates (96 wells; Nunc) at 30 °C for 48 h. Absorbance measurement at 620 nm (EZ Read 400, Biochrom) were taken at zero hour and at every 8 h for the following 48 h. Yeast growth controls without addition of peptides were also determined. Assays were performed in triplicate.

Yeast Cell Viability Assay

To evaluate whether the inhibition of yeast growth was caused by the fungistatic or fungicidal effect of the peptides, the control cells (without peptide treatment) and treated cells (with 200 μg mL^{-1} peptide treatment for 24 h) were washed and diluted 1000-fold. An aliquot of yeast cells were quantified in a Neubauer chamber and an aliquot with 10^2 cells mL^{-1} was spread with a Drigalski spatula on the surface of a Petri dish containing Sabouraud agar and grown at 30 °C for 48 h. After this period, the colony-forming units were quantified and Petri dishes were photographed. The assays were performed in triplicate, and the results are presented assuming that the control represents 100% cell viability.

Cell Death Monitoring Assays and Plasma Membrane Permeabilization

Cell death monitoring was done by propidium iodide (PI) staining and the plasma membrane permeabilization of cells was measured by Sytox green uptake, according to the methodology described by Deere et al. [43] and by Thevissen et al. [44], respectively. Yeasts cells were incubated with peptides (200 μg mL^{-1}) for 24 h. After this time, a 100 μL aliquot of each yeast cell suspension was incubated with 0.5 μg mL^{-1} of PI and 0.2 μM of Sytox green in 1.5 mL microcentrifuge tubes for 10 min at 25 °C. Cells were analyzed by DIC optical microscope (Axiovison 4, Zeiss) equipped with a fluorescent filter set for detection of the PI (excitation wavelength, 561 nm, emission wavelength 630 nm) and for detection of fluorescein (excitation wavelength, 450–490 nm, emission wavelength 500 nm). Negative controls (untreated yeast cells) were also done to determine the baseline level of membrane permeability and cell death. Cell counts were performed using the ImageJ software tool [45]. The results represent triplicate experiments.

Increase of Intracellular ROS Detection

To determine whether the mechanism of action of peptides involves cell oxidative stress, the fluorescent probe 2,7-dichlorofluorescein diacetate (H_2DCFDA) was used to measure intracellular reactive oxygen species (ROS) according to the protocol described by Mello et al. [46]. Yeast cells were incubated with peptides (200 μg mL^{-1}) for 24 h and after this time, 100 μL of yeast cell suspension was incubated with 50 μM of H_2DCFDA in microcentrifuge tubes of 1.5 mL for 30 min at 25 °C. Yeast cells were visualized by DIC optical microscope (Axiovison 4, Zeiss) equipped with a fluorescent filter set for detection of the fluorescein (excitation wavelength 450–490 nm, emission wavelength 500 nm). Cell counts were performed using the ImageJ software tool [45]. The experiments were performed in triplicate.

Metacaspase Activity Detection

Metacaspase activity detection was performed using the CaspACE FITC-VAD-FMK marker (Promega) as described by the manufacturer. Yeast cells were incubated with peptides (200 μg mL^{-1}) for 24 h and after this incubation, an aliquot of 100 μL of yeast cell suspension was incubated for 20 min at 30 °C with 0.5 μL of probe solution (supplied by the kit) containing 50 μM of the FITC-VAD-FMK marker. Cells were analyzed by DIC using an optical microscope equipped with a fluorescence filter to detect fluorescein (excitation wavelength 450–490 nm, emission wavelength 500 nm). Cell counts were performed using the ImageJ software tool [45]. The experiments were performed in triplicate.

Enzymes Inhibition Assays

The enzymatic activity assay for *Tenebrio molitor* α-amylase and human salivary α-amylase (EC 3.2.1.1) was performed as previously described by Bernfeld [47]. Activity assay for porcine pancreatic α-amylase was done with the same method, but using PBS buffer. Peptides at increasing concentrations were incubated with 10 U of α-amylase, and each enzyme mixture was equilibrated in a water bath for 15 min at 37 °C. After that, 25 μL of 1% starch solution (Sigma-Aldrich Co.) were added, and the samples were incubated in a water bath at 37 °C for 30 min. The samples were removed from the water bath and mixed with 400 μL of 3.5 dinitrosalicylic acid (DNS). Each sample was boiled for 5 min and, after cooling, mixed with 400 μL of water. Substrate hydrolysis was determined by absorbance reading at 540 nm (Chameleon V, Hidex). EDTA (5 mM) was used as a negative control. All inhibition assays were performed in triplicate and the results were shown in activity relative to the positive control (100% activity).

Trypsin and chymotrypsin inhibitory activities were quantified by measuring the hydrolytic activity of porcine trypsin and bovine chymotrypsin toward the substrates BapNa (*N*-benzoyl-Dl-arginyl-*p*-nitroanilide) and BatNa (*N*-benzoyl-L-tirosil-*p*-nitroanilide) respectively. Inhibitory activity was determined by incubating peptides at increasing concentrations from 25 to 300 μg mL^{-1} with enzymes and their respective substrates in 50 mM Tris–HCl buffer (pH 8.0) at 37 °C in a final volume of 200 μL. A control sample without peptides was included in each assay. The reaction was stopped with 100 μL of 30% (v/v) acetic acid. Substrate hydrolysis was quantified by measuring the absorbance of *p*-nitroaniline at 405 nm [48]. All inhibition assays were

performed in triplicate and the results were shown in activity relative to the positive control (100% activity).

Papain inhibitory activity was performed according to Michaud et al. [49] with modifications, using azocasein as substrate. Azocasein 1% was prepared as solution in citrate–phosphate buffer (100 mM sodium citrate pH 5.6; 100 mM sodium phosphate, 0.1% triton X-100, and 1.5 mM DTT). *Ca*CPin-II at increasing concentrations from 30 to 240 μg mL^{-1} were incubated with papain (Fluka) 10 μg mL^{-1} and azocasein solution to a final volume of 120 μL. Samples were incubated at 37 °C for 1 h. The reaction was stopped with 300 μL of 10% trichloroacetic acid (TCA). Samples were centrifuged at 2000 × *g* for 5 min. To the supernatant were added 300 μL of NaOH 1 M. The absorbances were measured at 440 nm. All inhibition assays were performed in triplicate and the results were shown in activity relative to the positive control (100% activity).

Hemolytic Activity

Peptides hemolytic activity was measured using defibrinated sheep red blood cells (sRBC) according to the methodology described by Oren and Shai [50] with modifications. Fresh defibrinated sRBC with EDTA were washed with saline solution (0.15 M NaCl) by centrifugation for 10 min at 2400 × *g* and resuspended in saline solution (final erythrocyte concentration, 1% v/v). The peptides dilutions were prepared in microtubes containing saline solution. Then, peptides at concentrations of 400, 200, and 100 μg mL^{-1} (50 μL) were incubated with sRBC suspension (50 μL) at 37 °C for 1 h. After this incubation time, the samples were centrifuged at 2400 × *g* for 10 min, and the supernatant was transferred to a well in a 96-well microplate. Free hemoglobin content was measured by absorbance at 405 nm. Positive hemolysis control (C^+) was performed using a solution containing 1% Triton X-100 and a negative hemolysis control (C^-) was performed using erythrocytes in saline. Hemolytic activity percentual was calculated assuming that the positive control represents 100% hemolysis according to the formula: % of hemolytic activity = $100 \times (\text{peptide}_{ABS405} - C^-_{ABS405})/(C^+_{ABS405} - C^-_{ABS405})$. The 50% cytotoxic concentration (CC_{50}) was defined as the concentration of peptide (μg mL^{-1}) that caused 50% hemolysis and was estimated by nonlinear regression of a log (inhibitor) vs. normalized response equation to the experimental data. The results shown are average values obtained in three experiments, performed in triplicate. Dose–response curves were constructed.

Statistical Analysis

Statistical analysis was carried out with GraphPad Prism software (version 8.0 for Windows) and one-way analysis of variance (ANOVA); $p < 0.05$ was considered statistically significant. The half maximal inhibitory concentration (IC_{50}) values were calculated by nonlinear regression of a log (inhibitor) vs. normalized response equation to the experimental data.

Results

Purification and Characterization of Peptides from *C. annuum* Leaves

Extracts from *C. annuum* leaves were separated into three fractions using reversed-phase chromatography: peak 0 (P_0), peak 1 (P_1), and peak 2 (P_2) (Fig. 1). On gel electrophoresis, the three fractions presented a single band each with a molecular mass between 3.5 and 6.5 kDa (Fig. 1 insert).

The 35 amino acid residues of the band obtained from fraction P_0 (Fig. 2A), termed *Ca*CPin-II (RLCTNCCAGRKGCNYYSADGTFICEGESDPNNPKA), were compared with a specific Pin-II type protease inhibitor database and revealed 100% similarity with the primary structure of some inhibitory repeated domains (IRDs), such as IRD 100, IRD 118, IRD 84, and IRD 85, all of them from *C. annuum*. The 29 amino acid residues of the band obtained from fraction P_1 (Fig. 2B), termed *Ca*CDef-like (VPTTPFLCTNDPQCK—-VNYEDGHCFDILSK), were compared with the protein database and revealed 85, 85, 85, and 82% similarity with the primary structure of plant AMPs stress-induced peptide from *C. annuum* (ID: AHI85724.1), flower specific defensin-like peptide from *C. annuum* (ID: XP_016579689.1), defensin-like hypothetic protein from *C. annuum* (ID: KAF3614338.1), and defensin-like hypothetic protein from *C. chinense* (ID: PHT96586.1), respectively. The sequence of 33 amino acid residues of the band from fraction P_2 (Fig. 2C) were named *Ca*CLTP2 (GQQSCLCGYM—-KQYVNSPNARKVVGQCGVSVPNC), and revealed 87, 82, 82, and 55% similarity with the primary structure of plant AMPs belonging to the non-specific lipid transfer proteins type 2 class (nsLTP2) peptides from *C. annuum* (ID: KAF3615994.1), *C. annuum* (ID: KAF3615995.1), *C. baccatum* (ID: PHT56658.1), and *C. chinense* (ID: PHU06864.1), respectively. Homology modeling of *Ca*CPin-II, *Ca*CDef-like, and *Ca*CLTP2 protein tertiary structures is shown in Fig. 3A–C. Homology modeling of *Ca*CPin-II structure showed that it was composed only of a β-sheet with four antiparallel strands. *Ca*CDef-like protein had a compact globular structure consisting of an α-helix and a β-sheet composed of three antiparallel strands, in a βαββ configuration. The spatial structure of *Ca*CLTP2 included three α-helices and a region containing single helical coils. The first and second helices were arranged parallel to each other, and the third helix was formed at an angle of 90° with respect to the second helix. Red regions represent signal peptides. Circular

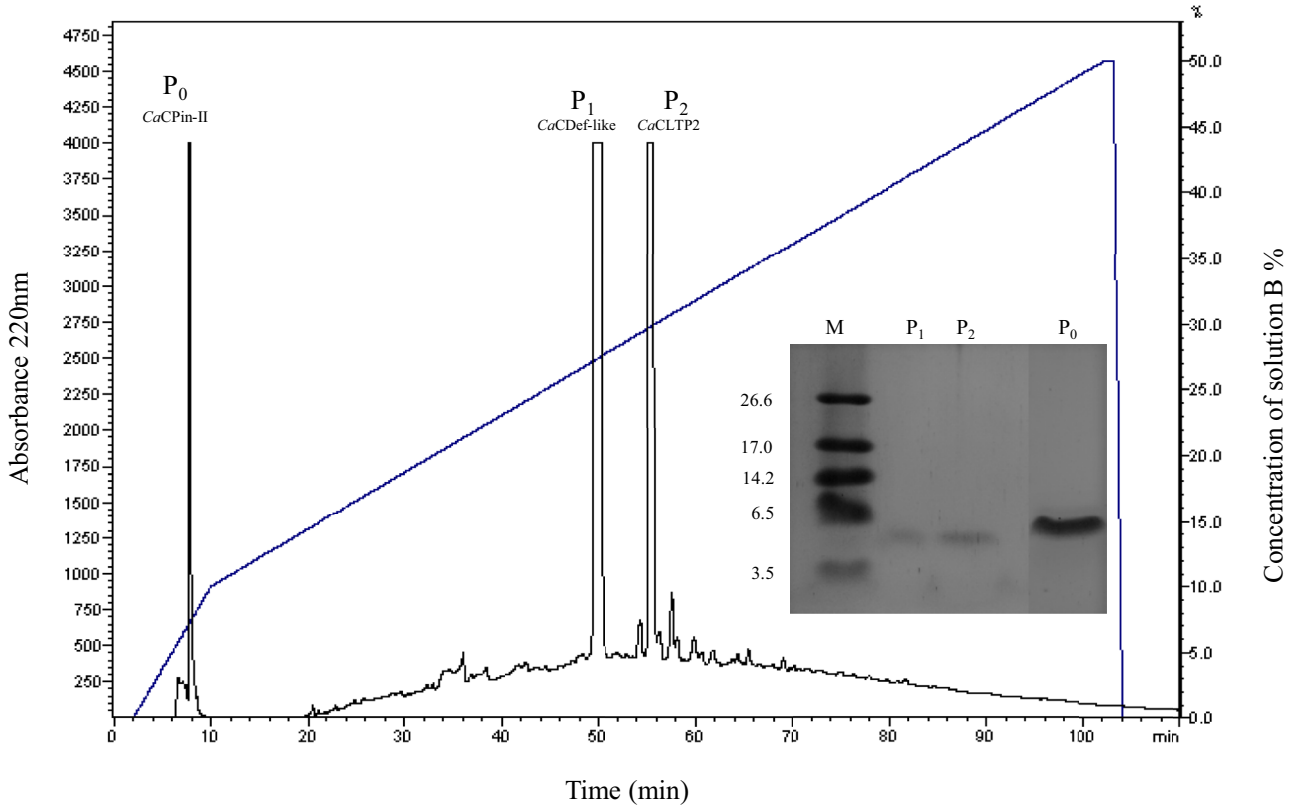

Fig. 1 Fractionation of *C. annuun* extract. Chromatogram of the extract of *C. annuum* leaves in reversed-phase C_{18} column. The column was equilibrated and eluted with 0.1% trifluoroacetic acid (TFA) (solution A) and eluted using a gradient of 90% acetonitrile in 0.1% (solution B). The flow used was 0.5 mL min^{-1}. (Insert) Fractionation in a SDS-tricine-gel of peptides enriched fractions obtained by the fractionation of the extract of *C. annuum* leaves (cv. Carioquinha) by reversed-phase C_{18} column in HPLC. **P_0** Peak 0 (*Ca*CPin-II). **P_1** Peak 1 (*Ca*CDef-like). **P_2** Peak 2 (*Ca*CLTP2). **M** Molecular mass (kDa) markers: 26.6, 17.0, 14.2, 6.5 and 3.2 kDa

dichroism spectroscopy of the *Ca*CDef-like and *Ca*CLTP2 peptides (Fig. 3E) revealed a random coil structure compatible with the structure predicted by homology modeling (Fig. 3B, C). However, circular dichroism spectroscopy of the *Ca*CPin-II peptide revealed a secondary structure pattern different from that of the β-sheet-rich structure predicted by homology modeling (Fig. 3A). Therefore, we performed structural modeling of one of the 35 amino acid residue fragments identified in *Ca*CPin-II (Fig. 3D). This fragment was modeled with 99.9% confidence using the single highest-scoring template. In the structure predicted for this fragment, a disordered conformation predominated, also containing a β-sheet and an α-helix, which is consistent with the circular dichroism results.

Antifungal Activity of the Peptides Against *Candida* Species

To analyze the effect of peptides on the growth of yeasts *C. albicans*, *C. buinensis*, *C. tropicalis*, and *C. parapsilosis*, we used *Ca*CPin-II, *Ca*CDef-like, and *Ca*CLTP2 at increasing concentrations from 1.56 to 200 μg mL^{-1} (Fig. 4). *Ca*CPin-II inhibited *C. albicans* growth at all concentrations, reaching 39% inhibition at the concentration of 200 μg mL^{-1}. However, no significant difference was observed between 25 and 200 μg mL^{-1} (i.e., inhibition was not dose-dependent). *C. buinensis* growth showed 37 and 70% inhibition at concentrations of 100 and 200 μg mL^{-1}, respectively, and the IC_{50} value for *C. buinensis* was 54.2 μg mL^{-1}. *Ca*CPin-II had no significant effect on the growth of *C. tropicalis* or *C. parapsilosis* at any of the concentrations tested. *Ca*CDef-like peptide also inhibited the growth of *C. albicans* at all tested concentrations, with no dose-dependent effect, reaching 44% inhibition at 50 μg mL^{-1}, although there was no significant difference between 200 and 3.12 μg mL^{-1}. The growth of *C. buinensis* and *C. tropicalis* was not significantly affected by *Ca*CDef-like at the concentrations tested, while that of *C. parapsilosis* was inhibited by only 10% at 50 μg mL^{-1}. *Ca*CLTP2 peptide also inhibited the growth of *C. albicans* at all tested concentrations with no dose-dependent effect, reaching 45% inhibition at 200 μg mL^{-1}, and there was

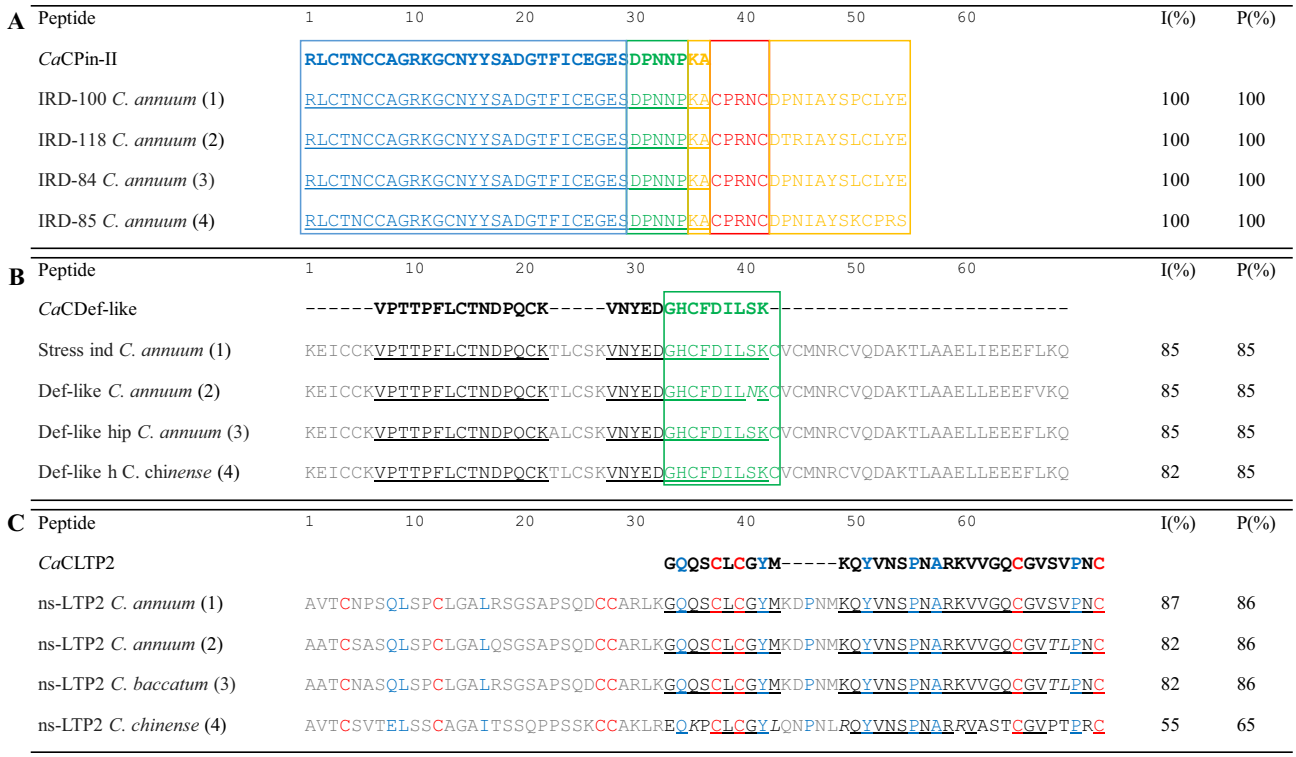

Fig. 2 **A** Alignment of the 35 amino acid residues obtained from the peptide of the P_0 fraction with the following peptide sequences similar to the inhibitory repeated domains (IRDs) from Pin-II type protease inhibitor. Heavy chain amino acids residues are color-coded in blue, linker region (DPNNP) is color-coded in green, light chain amino acids residues are color-coded in yellow with the reactive center loop (RCL) highlighted in red. **B** Alignment of the 29 amino acid residues obtained from the peptide of the P_1 fraction with the following peptide sequences similar to the defensins-like. The green highlighted region represents the γ-core motif (GXCX3-9C). *C. annuum* stress induced protein (1) (ID: AHI85724.1). *C. annuum* flower specific defensin-like, predicted protein (2) (ID: XP_016579689.1). *C. annuum* defensin-like, hypothetic protein FXO38_35740 (3) (ID: KAF3614338.1). *C. chinense* defensin-like, hypothetic protein BC332_34488 (4) (ID: PHT96586.1). **C** Alignment of the 33 amino acid residues obtained from the peptide of the P_2 fraction with the following peptide sequences similar to the ns-LTP2. The cysteines highlighted in red represent the 8-cysteine motif found in LTP2. Residues highlighted in blue are those highly conserved in LTP2. *C. annuum* ns-LTP2 (1) (ID: KAF3615994.1). *C. annuum* ns-LTP2 (2) (ID: KAF3615995.1). *C. baccatum* ns-LTP2 (3) (ID: PHT56658.1). *C. chinense* ns-LTP2 (4) (ID: PHU06864.1). I% indicates the percentage of identical residues and amino acids highlighted in underline (including Cys residues). P% indicates the percentage of positive amino acid residues (with the same physicochemical characteristics) highlighted by italicized. I% and P% were made based on the amino acids of the tryptic fragments obtained in mass spectrometry. Spaces (-) have been introduced for better alignment. The numbers above the sequence indicate the size of the peptides in amino acid residues. The sequences shown were obtained from Blast-p (b/c) and from Pin-II type PIs Information Resources (PINIR) (a), and aligned using Clustal Omega

no significant difference in inhibition between 200 and 3.12 μg mL^{-1}. *Ca*CLTP2 at the concentrations tested did not significantly affect *C. tropicalis* and *C. parapsilosis* growth and inhibited only 18% of the *C. buinensis* growth.

The viability assay (Fig. 5) demonstrated that the species most susceptible to *Ca*CPin-II were *C. albicans* and *C. buinensis*, with viability losses of 38.3 and 96.6%, respectively. *C. albicans*, *C. buinensi*, and *C. parapsilosis* were susceptible to *Ca*CDef-like, with approximately 37% viability loss, and the species most susceptible to *Ca*CLTP2 were *C. albicans* and *C. buinensis*, with viability losses of 49.6 and 66.2%, respectively. These data suggest that the inhibitory effect of the peptides is fungistatic but *Ca*CPin-II (200 μg mL^{-1}) is lethal to 96.6% of *C. buinensis* yeasts.

Toxic Effects of Peptides Against Yeasts

The antifungal effects of the peptides were characterized with respect to their mechanism of action. For this purpose, fluorescent probes were used (Table 1). Because the effects of the peptides on the different *Candida* species were similar, microscopic photos of *C. buinensis* are presented in Fig. 6, and those of *C. albicans*, *C. tropicalis*, and *C. parapsilosis* are presented in Supplementary Information.

C. albicans, *C. buinensis*, *C. tropicalis*, and *C. parapsilosis* were used to test membrane permeabilization using a SYTOX Green probe after 24 h in the presence of the peptides (200 μg mL^{-1}). *Ca*CPin-II and *Ca*CDef-like proteins induced membrane permeabilization. *Ca*CLTP2 was not significantly

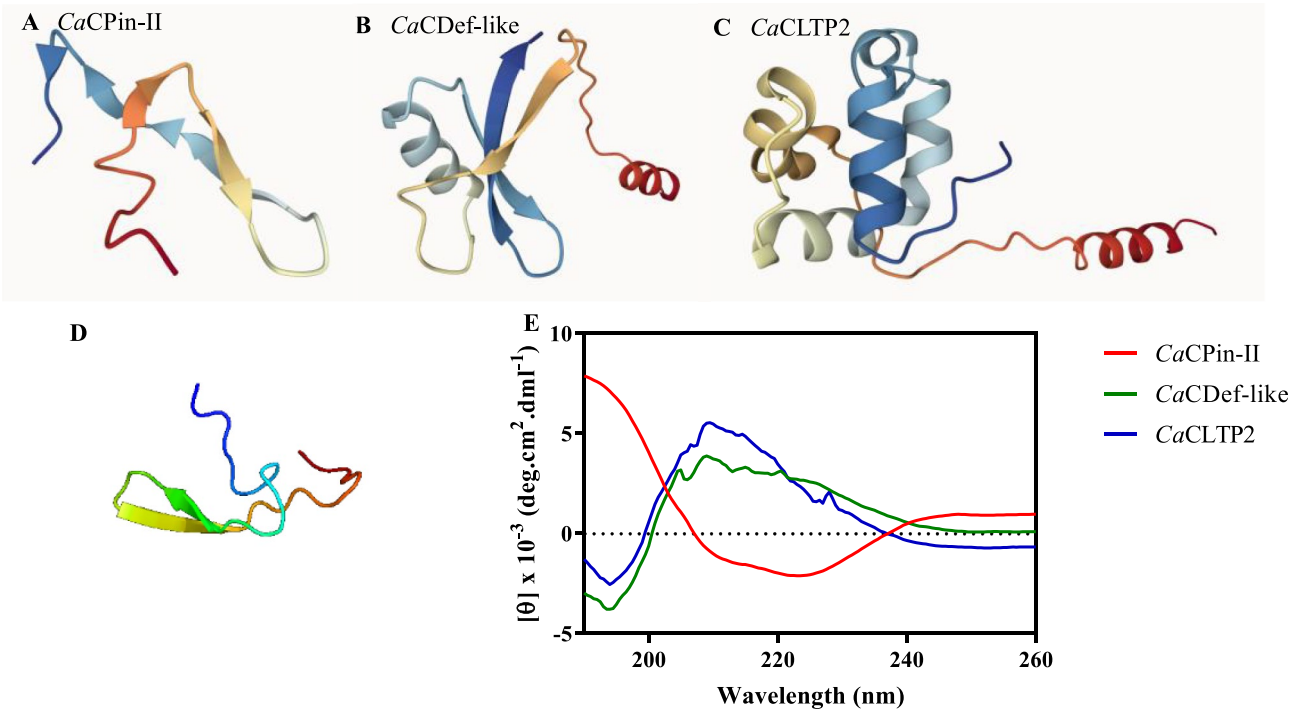

Fig. 3 Tertiary and secondary structures of peptides. Homology modeling of protein tertiary structures of *Ca*CPin-II (**A**), *Ca*CDef-like (**B**), and *Ca*CLTP2 (**C**) from *C. annuum* leaves. These sequences were searched against the AlphaFold DB (Jumper et al. 35) using the EBI Protein Similarity Search tool (https://www.ebi.ac.uk/Tools/sss/fasta/). The AlphaFold model of sequence P56615 (Pin-II) and of the best orthologs (Q9FFP8 for defensin and A0A0R0FHG0 for nsLTP2) were used as templates for homology modeling with Phyre2 (Kelley et al. 36) using one-to-one threading mode. **D** Modeling of one of the 35 amino acid residue fragments of *Ca*CPin-II. **E** Secondary structure of *Ca*CPin-II (red line), *Ca*CDef-like (green line), and *Ca*CLTP2 (blue line). Circular dichroism (CD) spectra of 200–400 µg mL^{-1} peptide solutions prepared in ultra-pure water

effective in permeabilizing the membranes of the tested yeasts. This assay showed that *Ca*CPin-II and *Ca*CDef-like peptides could compromise the structure of the plasma membrane, as shown in Fig. 6A for *C. buinensis*, possibly causing the membrane to be permeable enough for the probe to enter the cells; however, this effect was not observed in *C. albicans* and *C. parapsilosis* cells (Supplementary Information).

We also observed using DIC microscopy that in the presence of peptides, yeast growth displayed morphological changes that were not observed in the controls, such as cell agglomeration, increased cell volume, vacuole formation, difficulty in bud liberation, and the emergence of pseudohyphae.

The effect of peptides on the induction of ROS production in different species of *Candida* resulted in labeling with the probes of *C. buinensis* grown in the presence of *Ca*CPin-II (10.6% of cells) (Fig. 6B) and *C. tropicalis* cells grown in the presence of *Ca*CPin-II and *Ca*CDef-like (30.0 and 44.6% of cells respectively) (Table 1). Positive labeling was also observed for *C. parapsilosis*, but it was less intense. These results indicated increased ROS production in these yeasts. The same effect was not observed in *C. albicans* treated with the same peptides. *Ca*CLTP2 induced less intense ROS production in *C. parapsilosis* and *C. albicans* than the other tested peptides.

The rate of yeast cell death was determined using a propidium iodide assay with 200 µg mL^{-1} peptides. The cells labeled with the SYTOX probe was the same labeled with propidium iodide, as shown for *C. buinensis* in Fig. 6. *Ca*CPin-II caused 20 and 25% cell death in *C. buinensis* and *C. tropicalis* respectively, whereas *Ca*CDef-like and *Ca*CLTP2 only caused 20% cell death in *C. tropicalis* (Table 1). To determine if apoptosis-like programmed cell death (PCD) was the cause of cell death, we performed metacaspase activity detection (Fig. 6C). *Ca*CPin-II induced metacaspase activity in approximately 9 and 16% of *C. buinensis* and *C. tropicalis* cells, respectively, while *Ca*CDef-like and *Ca*CLTP2 respectively induced metacaspase activity in 19 and 12% of *C. tropicalis* cells (Table 1). Collectively, these results suggest that apoptosis-like PCD might be involved in cell death in these cases.

Effects of Peptides on α-Amylase and Protease Activities

To elucidate the toxic effects of the peptides against yeasts, we investigated their capacity to inhibit hydrolases. *Ca*CPin-II inhibited *T. molitor* α-amylase (Fig. 7A), human salivary

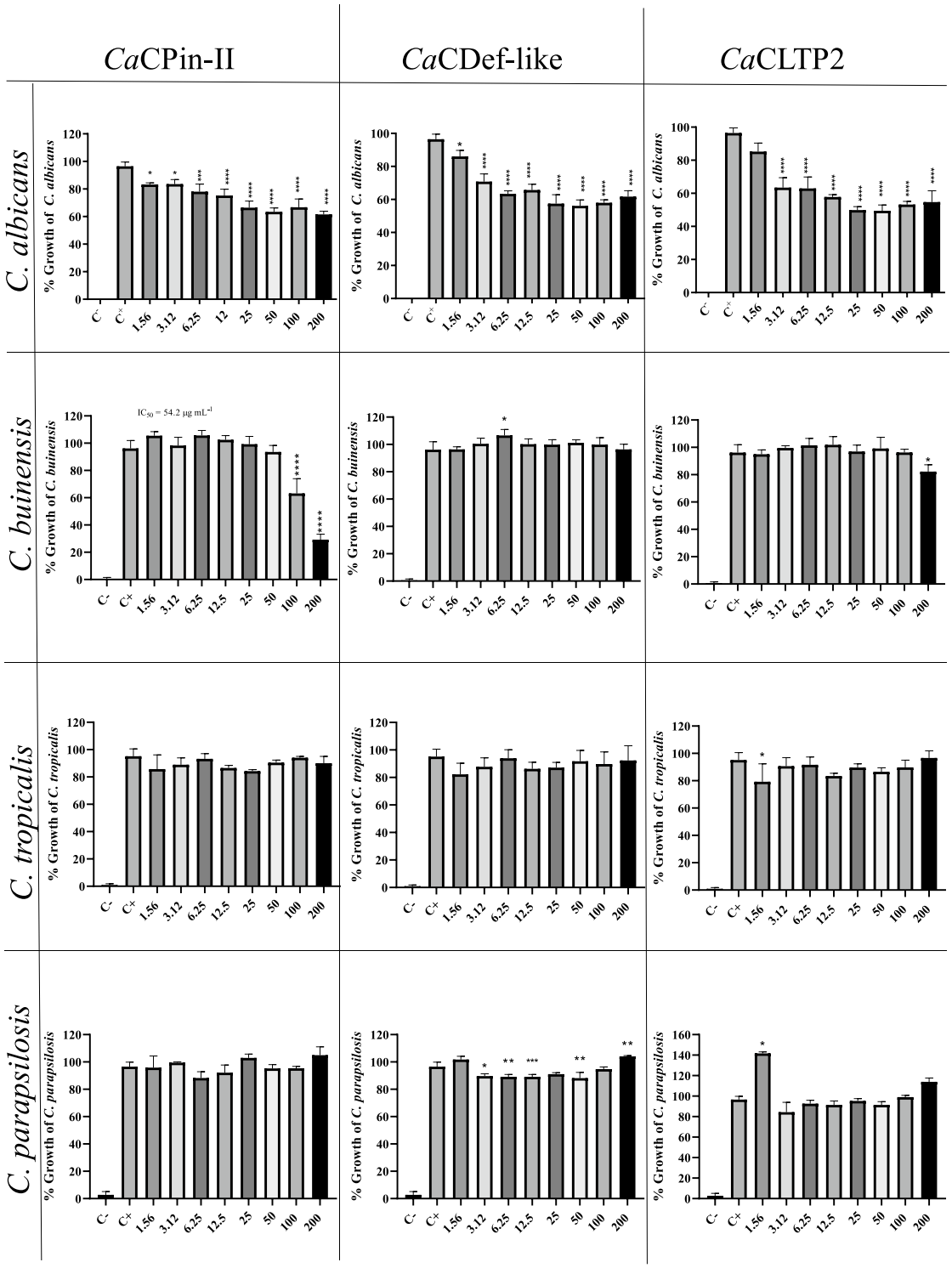

Fig. 4 Effect of peptides on yeast growth. Yeasts suspensions (1×10^4 cell mL^{-1}) of *Candida* sp. were treated or untreated with *Ca*CPin-II, *Ca*CDef-like, and *Ca*CLTP2 from *C. annuum* leaves (200, 100, 50, 25, 12.5, 6.26, 3.12, or 1.56 µg mL^{-1}) for 24 h. Yeasts growth in the resulted cultures was quantified by optical density (620 nm). Data are presented as a percentage of yeasts growth of treated culture compared to the growth of corresponding untreated culture (100%). Negative control (C^-)- Sabouraud Broth; positive Control (C^+) untreated yeasts suspensions. The results presented are mean values obtained over three experiments, each done in triplicate. Dose response curves were constructed and $^*p < 0.05$; $^{**}p < 0.01$; $^{***}p < 0.001$; $^{****}p < 0.0001$ compared to positive control (0 µg mL^{-1}) determined by Tukey test

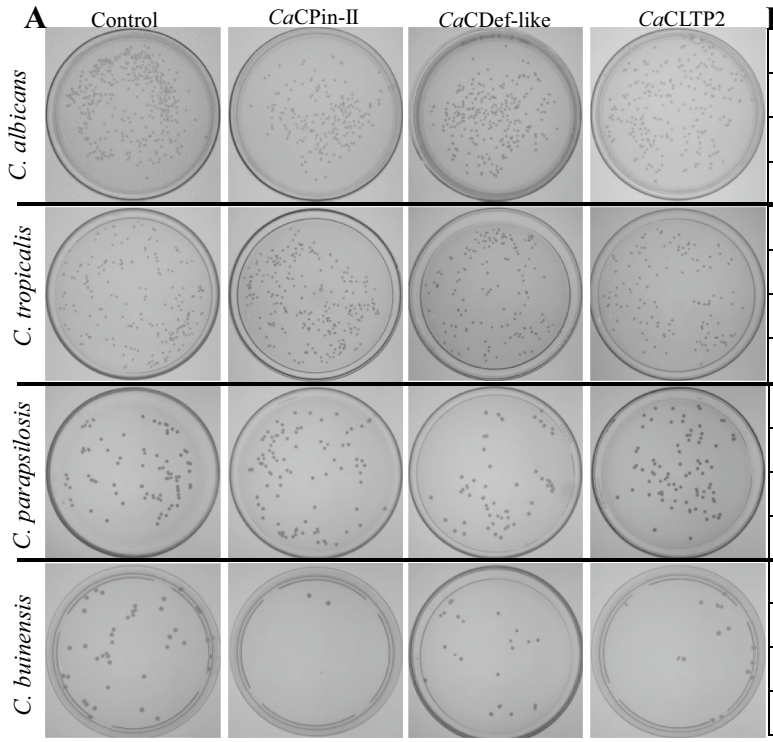

B

Peptide	CFU	Viability loss (%)
Control	364.5 ± 10.6	0
*Ca*CPin-II	229.5 ±23.3	38.3**
*Ca*CDef-like	237.0 ±24.0	36.3*
*Ca*CLTP2	187.5 ±19.1	49.6**
Control	157.7 ±15.4	0
*Ca*CPin-II	193.0 ±18.5	0
*Ca*CDef-like	140.3 ±16.4	11.0
*Ca*CLTP2	115.0 ±24.9	27.1
Control	88.0 ±3.5	0
*Ca*CPin-II	81.3 ±15.0	7.6
*Ca*CDef-like	55.7 ±7.0	36.7*
*Ca*CLTP2	72.7 ±19.7	17.42
Control	44.3 ±7.5	0
*Ca*CPin-II	1.5 ±0.7	96.6***
*Ca*CDef-like	28.0 ±6.6	36.8*
*Ca*CLTP2	15.0 ±3.0	66.2***

Fig. 5 Cell viability. **A** Photographs of the Petri dishes for analysis of yeasts cells viability after the treatment with *Ca*CPin-II, *Ca*CDef-like, and *Ca*CLTP2 (200 µg mL^{-1}) for 24 h. **B** Table presenting the percentage of viability loss of yeast cells after the treatment with *Ca*CPin-II, *Ca*CDef-like, and *Ca*CLTP2 (200 µg mL^{-1}) for 24 h. Colony-forming unit (CFU). The experiments were carried out in triplicate and $*p<0.05$; $**p<0.01$; $***p<0.001$ compared to control (untreated) determined by *t* test

α-amylase (Fig. 7B), and porcine pancreatic α-amylase (Fig. 7C), with an IC_{50} of 19.4 µg mL^{-1}, 4.9 µg mL^{-1}, and 1.8 µg mL^{-1}, respectively. *Ca*CDef-like and *Ca*CLTP2, at the same concentrations, were unable to inhibit α-amylases (data not shown). We also tested the ability of these peptides to inhibit protease activity. None of the peptides inhibited the serine proteases trypsin and chymotrypsin at concentrations up to 300 µg mL^{-1} (data not shown). Because *Ca*CPin-II shares identities with protease inhibitor peptides, we tested its ability to inhibit cysteine proteases. This peptide inhibited papain (Fig. 7D) with an IC_{50} of 84.36 µg mL^{-1}. These data suggest that the ability to inhibit α-amylase and cysteine proteases may be related to the toxicity of CaCPin-II against yeasts.

Hemolytic Activity

To evaluate the possibility that the inhibitory effects of the peptides against *Candida* species were associated with toxicity in mammalian cells, we monitored the hemolytic activity against defibrinated sheep red blood cells. *Ca*CPin-II showed hemolytic activity at a concentration of 200 µg mL^{-1}, causing 28% hemolysis ($p<0.0001$ compared to the positive control). The *Ca*CPin-II CC_{50} was calculated as 270 µg mL^{-1} (Fig. 8A). *Ca*CDef-like had no hemolytic effect at concentrations up to 400 µg mL^{-1} ($p<0.0001$ compared with the positive control) (Fig. 8B), and *Ca*CLTP2 showed a weak hemolytic effect at a concentration of 200 µg mL^{-1}, causing 1.7% hemolysis and presenting a $CC_{50}>400$ µg mL^{-1} ($p<0.0001$ compared with the positive control) (Fig. 8C).

Discussion

Over the past 20 years, many AMPs have been purified and characterized from numerous plants [51, 52], including hot pepper (*C. annuum*), a species with well-described medicinal importance [18]. Some peptides purified from hot peppers show antifungal activity, including a thionin-like peptide with activity against *C. albicans* and *C. tropicalis* [25], defensins with activity against *Candida* species [19], LTP-1 with activity against *C. tropicalis* [53], and a hevein-like peptide with activity against *Fusarium oxysporum* and *Colletotrichum gloesporioides* [54]. However, the mechanism of action of plant antimicrobial peptides against pathogens requires further investigation. We isolated and characterized three peptides from *C. annuum* leaves that caused a considerable increase in the incidence of *Candida* spp.

Table 1 Cell density and fluorescent cell percentage of *Candida* sp. treated with *Ca*CPin-II, *Ca*CDef-like, and *Ca*CLTP2 peptides from *Capsicum annuum* leaves

Yeast	Treatment	Cell count in DIC[a]	Cell count in flourescence (PI)[a] and % of fluorescense cells[b]		Cell count in fluorescence (Sytox)[a] and % of fluorescence cells[b]		Cell count in DIC[a]	Cell count in fluorescence (ROS)[a] and % of fluorescence cells[b]		Cell count in DIC[a]	Cell count in fluorescence (caspase)[a] and % of fluorescence cells[b]	
		a	a	b	a	b	a	a	b	a	a	b
C. albicans	Control	426.0 ± 31.3	1.8 ± 1.5	0.4	1.5 ± 1.3	0.4	137.4 ± 26.8	16.6 ± 11.8	12.1	73.4 ± 15.0	0.0 ± 0.0	0.0
	*Ca*CPin-II	475.3 ± 51.4	0.7 ± 0.6	0.1	1.3 ± 1.5	0.3	92.7 ± 46.6	3.0 ± 2.1	3.2	169.8 ± 10.1	0.0 ± 0.0	0.0
	*Ca*CDef-like	397.6 ± 53.9	2.8 ± 1.9	0.7	3.2 ± 1.3	0.8	162.6 ± 17.0	5.0 ± 2.1	3.1	100.4 ± 11.4	0.0 ± 0.0	0.0
	*Ca*CLTP2	483.0 ± 46.7	6.3 ± 1.5	1.3	6.5 ± 3.0	1.3	131.4 ± 12.7	8.0 ± 1.9	6.1	82.8 ± 15.3	0.0 ± 0.0	0.0
C. buinensis	Control	643.0 ± 116.3	11.0 ± 7.1	1.7	11.8 ± 4.8	1.83	261.0 ± 27.8	5.6 ± 2.9	1.6	117.4 ± 37.6	0.0 ± 0.0	0.0
	*Ca*CPin-II	35.0 ± 12.7	6.8 ± 4.1	19.5	6.8 ± 4.6	19.5	83.0 ± 30.9	8.7 ± 4.8	10.5	61.2 ± 12.8	5.4 ± 1.1	8.8
	*Ca*CDef-like	265.6 ± 5.8	4.4 ± 2.5	1.7	6.0 ± 2.5	2.3	120.8 ± 8.3	2.5 ± 1.7	2.1	101.0 ± 5.0	0.6 ± 0.9	0.6
	*Ca*CLTP2	203.8 ± 32.5	0.6 ± 0.9	0.3	0.6 ± 0.9	0.3	155.8 ± 23.2	3.2 ± 1.6	2.1	103.4 ± 7.8	0.0 ± 0.0	0.0
C. tropicalis	Control	72.2 ± 8.5	5.4 ± 7.8	7.5	8.0 ± 3.1	11.1	113.8 ± 26.6	14.0 ± 8.12	12.3	434.0 ± 82.6	3.6 ± 1.7	0.8
	*Ca*CPin-II	83.0 ± 8.2	21.0 ± 2.5	25.3	15.4 ± 3.2	18.6	127.6 ± 13.5	38.2 ± 9.6	30.0	446.6 ± 105.9	70.6 ± 29.8	15.8
	*Ca*CDef-like	113.7 ± 24.7	22.6 ± 8.3	19.9	21.7 ± 8.2	19.1	98.6 ± 24.1	44.0 ± 21.1	44.6	345.6 ± 50.1	65.4 ± 25.9	18.9
	*Ca*CLTP2	69.4 ± 8.0	14.2 ± 4.4	20.5	12.4 ± 5.0	17.9	74.6 ± 8.0	5.6 ± 3.6	7.5	477.2 ± 86.6	59.4 ± 10.0	12.4
C. parapsilosis	Control	170.8 ± 44.1	17.4 ± 2.7	10.2	17.6 ± 5.9	10.3	156.0 ± 12.8	1.4 ± 1.9	0.9	152.6 ± 16.8	0.6 ± 0.9	0.4
	*Ca*CPin-II	87.7 ± 8.5	5.5 ± 2.8	6.3	11.3 ± 3.3	12.9	109.6 ± 8.5	4.6 ± 2.9	4.2	89.2 ± 19.9	0.4 ± 0.5	0.4
	*Ca*CDef-like	95.2 ± 15.2	9.6 ± 2.9	10.1	12.4 ± 3.4	13.0	190.3 ± 28.8	15.8 ± 5.9	8.3	311.4 ± 43.5	1.0 ± 1.4	0.3
	*Ca*CLTP2	92.6 ± 18.4	6.8 ± 2.4	7.3	11.2 ± 4.3	12.1	145.5 ± 15.2	5.3 ± 2.9	3.7	210.2 ± 30.9	1.4 ± 1.9	0.7

[a]Cells number determination in five random fields of the DIC and fluorescence views of the samples obtained from microscopy assay

[b]The total cell number in DIC of each yeast (in control and test) was assumed as 100%

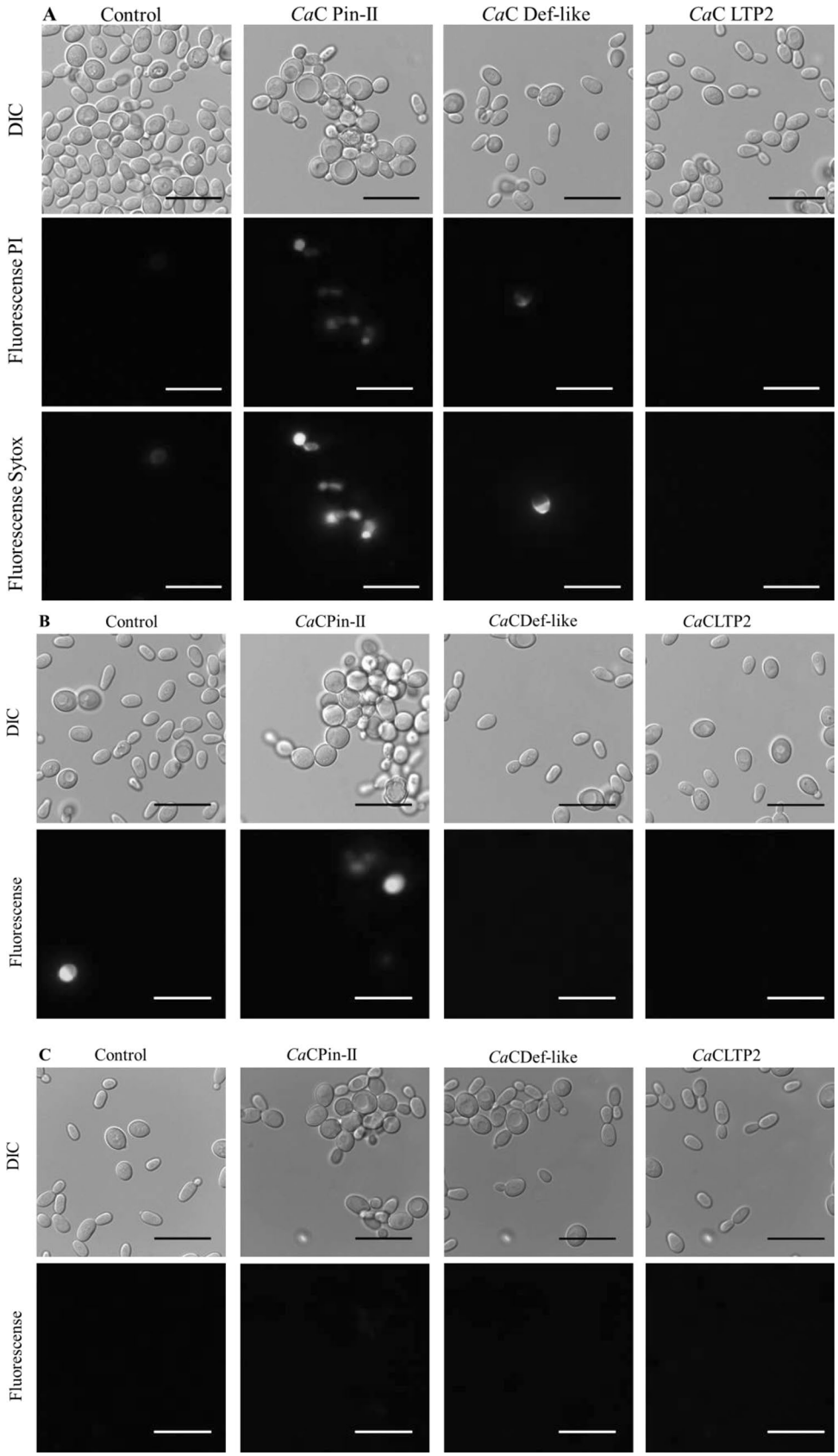

Fig. 6 Effect of the peptides in *C. buinensis*. Optical and fluorescence microscopy images of *C. buinensis* cells after treatment with peptides (200 µg mL^{-1}) for 24 h. **A** Images of cell death monitoring and membrane permeabilization assays. Control cells were treated only with propidium iodide (PI) stain or the SYTOX® Green probe. **B** Images of reactive oxygen species assay detection. Control cells were treated only with the 2′,7′-dichlorofluoresceindiacetate probe. **C** Images of metacaspase activity detection. Control cells and cells treated with peptides were incubated with the FITC-VAD-FMK probe and analyzed by fluorescence microscopy. Green fluorescence indicates positive staining for caspase activity. Bars = 20 µm. *DIC* differential interference contrast

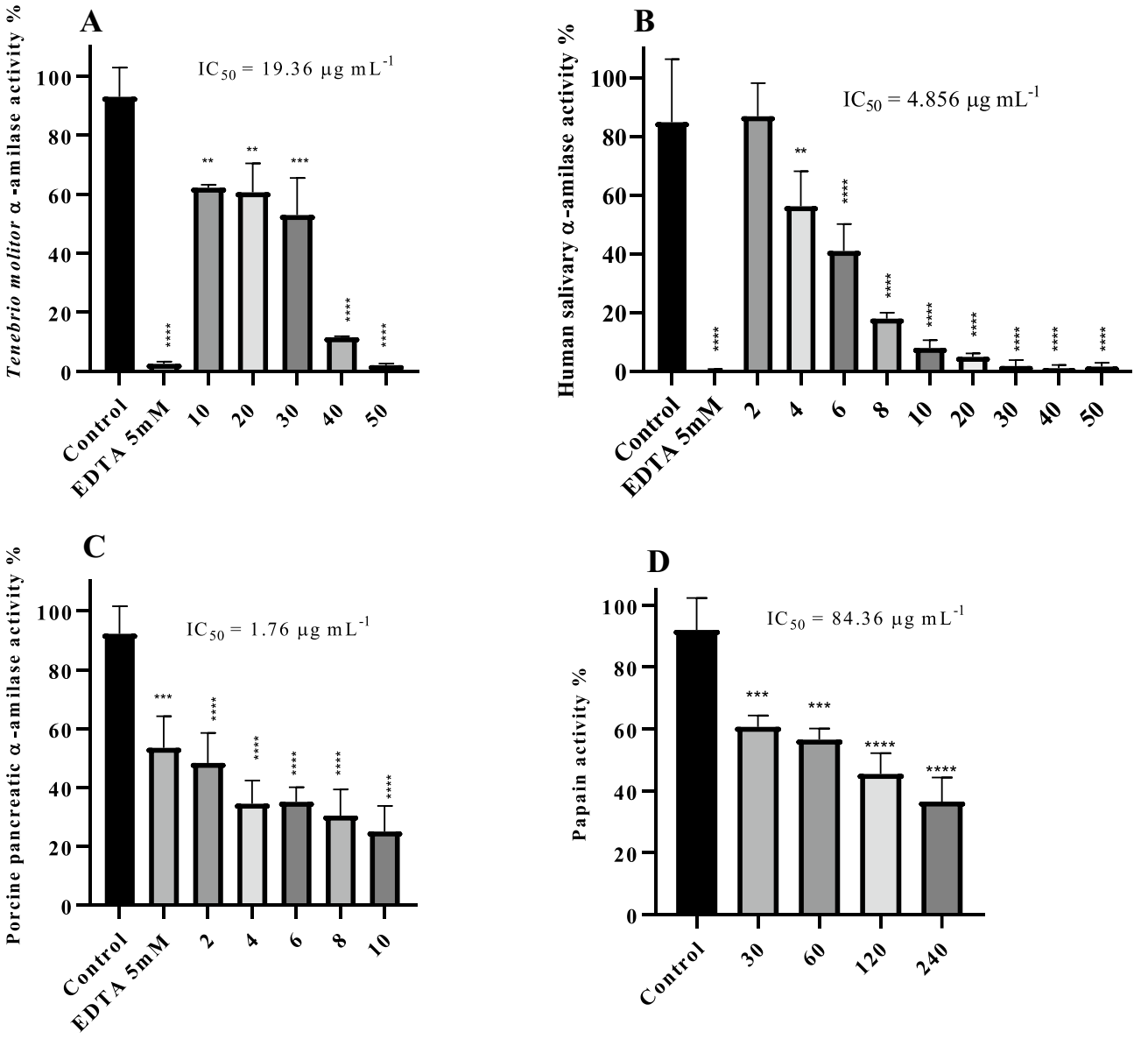

Fig. 7 Effect of *Ca*CPin-II on α-amylase and protease activities. Test with α-amylase from the intestine of *Tenebrio molitor* insects (**A**), from human saliva (**B**), and from pig pancreas (**C**); test with papain (**D**). Numbers below each bar indicate the peptide concentrations (µg $mL^{-.1}$). In the positive control of α-amylase inhibition, 5 mM EDTA was used. Asterisks indicate a significant difference when compared to the control by Tukey test, $^{**}p < 0.01$; $^{***}p < 0.001$; and $^{****}p < 0.0001$

infections in humans [55] and investigated their potential for the preparation of new drugs against four *Candida* strains of clinical interest: *C. albicans*, *C. buinensis*, *C. tropicalis*, and *C. parapsilosis*.

The three peptides from the leaf extracts obtained by C18 reversed-phase HPLC were named *Ca*CPin-II, *Ca*CDef-like, and *Ca*CLTP2 (*Ca*C = *Capsicum annuum* cv. Carioquinha) because of their amino acid sequence similarity to the inhibitory repeat domains (IRDs) of potato type inhibitor-II protease inhibitors, defensin-like protein, and non-specific lipid transfer protein type 2, respectively (Fig. 2). The spatial conformations determined by homology structure (Fig. 3A–C) were similar to those previously described in the literature [51, 56].

Pin-II-type proteinase inhibitors are serine proteinase inhibitors found mainly in solanaceous plants, with *C. annuum* having the highest number of sequences in the PINIR database [33]. This class of proteinase inhibitors plays a vital role in protecting plants against biotic stress [57], and has been used to develop antifungal agents [58, 59]. A single Pin-II-type proteinase inhibitor comprises multiple IRDs interspersed by 5 to 6 amino acid linker regions [56, 60]. The number of IRDs in a proteinase inhibitor varies, and the

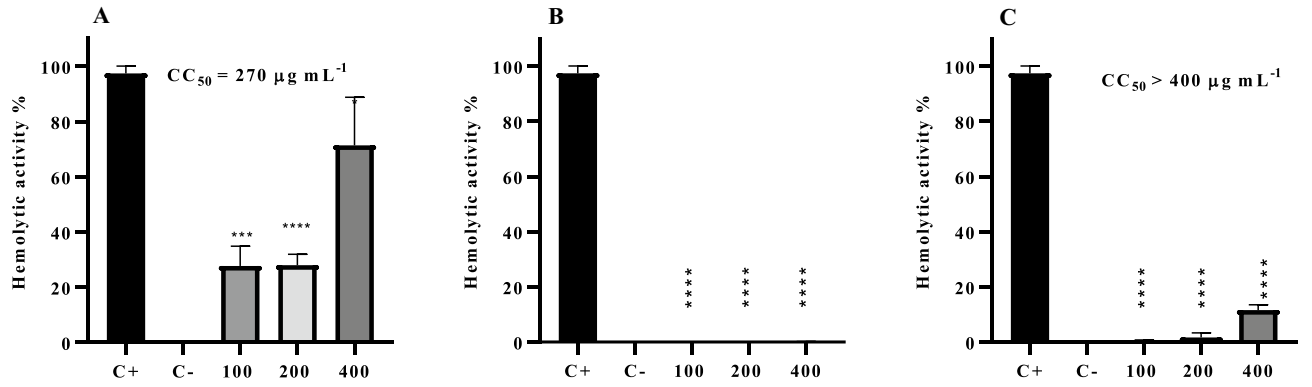

Fig. 8 Hemolytic activity of *Ca*CPin-II (**A**), *Ca*CDef-like (**B**), and *Ca*CLTP2 (**C**) from *C. annuum* leaves (400, 200, and 100 µg mL^{-1}). Test with defibrinated sheep red blood cells (sRBC). A solution containing 1% Triton X-100 was used as a positive hemolysis control (C^+) and erythrocytes in saline were used as a negative control (C^-). Asterisks indicate a significant difference when compared to the control by Tukey test, $*p < 0.05$; $***p < 0.001$; and $****p < 0.0001$

amino acid sequences of IRDs show subtle differences [61]. IRDs are 50–55 amino acid-long proteins, and proteolytic processing at linker regions releases IRDs from the parent Pin-II type proteinase inhibitor molecule [62, 63]. Each IRD is composed of a heavy and a light chain linked by a linker region. The light chain contains a tripeptide loop called the reactive center loop (RCL), which is the primary interaction site for the target serine protease and functions independently of the native IRD scaffold [33]. Due to this, the alignment of the P_0 amino acid sequence (Fig. 2A) was performed using a specific database for Pin-II type proteinase inhibitor, which contains amino acid sequences of the IRDs, since the BLASTp database contains only the parents Pin-II type proteinase inhibitor amino acid sequences. Secondary structure analysis of the *Ca*CPin-II peptide by circular dichroism spectroscopy was not compatible with the structure determined by homology modeling but was compatible with the modeling of the fragment of 35 amino acid residues (Fig. 3D, E). Therefore, we suggest that the *Ca*CPin-II peptide is smaller than Pin-II-type proteinase inhibitors described in the literature. This 35-residue fragment, despite having 100% similarity to Pin-II-type proteinase inhibitors, does not have all the necessary cysteines to form the four disulfide bridges found in this class of peptides, which explains its structure being different from that predicted. In addition, it lacks a large part of the light chain and the trypsin and chymotrypsin (RCL)-binding site, which explains why *Ca*CPin-II does not inhibit the activity of these enzymes.

Plant defensins play a role in both the response against pathogens and the control of plant growth and development [64], and their antifungal activity has been extensively described [19, 65]. The defensin signatures are a cysteine-stabilized αβ motif (CSαβ) and a γ-core motif GXC(X3–9)C [66], and peptides that contain variations in this typical structure are called defensin-like [67, 68], such as *Ca*CDef-like peptide. Nonspecific LTPs (nsLTPs) are a class of AMPs found in all land plants. LTPs have a tunnel-like hydrophobic cavity that enables them to bind and transport various types of lipids [69, 70]. In 2011, Edstam et al. classified plant LTPs into ten types based on the spacing between Cys residues in the eight-Cys motif (8CM), intron position, and polypeptide sequence identity. LTP2 is one of the most well-studied type [71, 72]. Several studies have demonstrated the toxicity of LTPs against fungal pathogens including *Candida* [22, 73–76]. Alterations in the fungal membrane permeability may be involved in the in vitro toxicity of LTPs [77].

Except for *C. albicans* and *C. buinensis* treated with *Ca*CPin-II, the other *Candida* species tested here did not show major growth alterations when treated with the *Ca*CPin-II, *Ca*CDef-like, and *Ca*CLTP2 peptides at concentrations up to 200 µg mL^{-1} (Fig. 4). These peptides caused morphological changes in the treated cells (Fig. 6), which might be related to the optical density values observed in the growth inhibition assays (Fig. 4). It has already been shown that a fraction rich in IRD-containing peptides from *C. chinensis* seeds caused morphological changes in *C. tropicalis*, including cellular agglomeration and formation of pseudohyphae [78]. We performed other assays to evaluate the effects of the peptides on the tested *Candida* species. *Candida albicans* and *C. buinensis* were the species with the greatest reduction in cell viability after treatment with 200 µg mL^{-1} peptides for 24 h, compared to *C. tropicalis* and *C. parapsilosis* (Fig. 5). The morphological changes and reduction in the density of *C. buinensis* cells treated with 200 µg mL^{-1} of *Ca*CPin-II seen in the microscopy images suggest that this peptide has a strong fungistatic effect that led to a 97% reduction in the viability of treated cells.

The membrane permeabilization assay with the SYTOX Green probe and the assay for labeling dead and damaged

cells with propidium iodide dye showed that, in some cases, the peptides permeabilized the yeast membranes, which may be related to the reduction in viability and cell death (Fig. 6A). Yeast membranes can be structurally compromised, leading to permeabilization. Labeling with propidium iodide is not specific for dead cells. This probe has been shown to label the membranes of stressed *S. cerevisiae* cells that have transient permeability, but are still viable [79]. The same cells stained with the SYTOX Green probe were also stained with propidium iodide, indicating that the damage was caused by membrane permeabilization (Fig. 6A). Plant defensins display several possible antifungal mechanisms such as cell membrane disruption and intracellular targets [80–82]. Other studies have shown that plant defensins can permeabilize cell membranes of microorganisms [19, 44, 46, 81]. AMPs may also have targets other than the cell membrane. *Ca*CLTP2 reduced the viability of *C. albicans* and *C. buinensis* (Fig. 5) without affecting membrane permeabilization (Fig. 6). The antimicrobial activity of some plant LTPs is found not to be related to their ability to interact with lipids, and it has been shown that this class of proteins may possess antimicrobial activity without binding lipid molecules [83, 84]. The mechanism of antimicrobial action of representatives of the LTP class remains unclear. Nevertheless, the cell membrane is considered a potential target for LTP antimicrobial action via electrostatic interactions that cause the destabilization and permeabilization of the membrane [85], as shown by the action of *Ca*CLTP2, which permeabilizes *C. tropicalis* membranes (Table 1).

Membrane permeabilization and increased ROS production are among the common modes of action of defensins and other AMPs, which might lead to PCD pathway activation [86, 87] and may be involved in the damage caused by peptides in these cells. Increased oxidative stress appears in the early stages of the apoptotic process [88], and the increased production of ROS molecules in target organisms is a recurrent mode of action employed by plant defensins and several other AMPs [46, 81]. Some *C. tropicalis* cells treated with *Ca*CPin-II and *Ca*CDef-like showed an increase in reactive oxygen species and the activation of metacaspases (Table 1), suggesting that the initial stages of apoptosis were in place.

To better understand the mechanism of action of the identified AMPs, we performed inhibition assays on several important enzymes such as proteases and amylases. Protease inhibitors, including fungal cells, affect gene expression, cell proliferation, and cell death [89], including fungal cells [90]. Several protease inhibitors affect fungal cells, leading to normal nutritional and/or growth functions. The mechanisms of action include membrane pore formation and/or cell wall disruption. These events disrupt ion flow and/or cause the leakage of internal cellular components, thereby affecting cell viability [91, 92]. Although the Pin-II type PIs are serine protease inhibitors, *Ca*CPin-II at concentrations up to 300 μg mL^{-1} and leaves extract at concentrations up to 1.200 μg mL^{-1} did not inhibit the tested serine proteases (data not shown). This fact, together with data from the secondary structure analysis of *Ca*CPin-II, suggests that this peptide lacks the binding site to cause the inhibition of serine proteases. Because *Ca*CPin-II was isolated from a *C. annuum* cultivar by genetic breeding [93], we suggest that the IRD precursor protein in this plant might be undergoing alternative proteolytic processing. However, the *Ca*CPin-II peptide showed cysteine protease activity and strong amylase inhibitory activity (Fig. 7). We suggest that *Ca*CPin-II is capable of inhibiting other serine proteases such as subtilisin, and/or that it is a new bifunctional inhibitor with activity against cysteine proteases and α-amylases. The combination of protease and α-amylase inhibition is potentially useful in plant defense and physiology [94, 95].

According to in silico tests, peptides are incapable of permeabilizing membranes (data not show). However, membrane permeabilization tests revealed positive labeling in some cells. This may be due to two hypotheses. First, the in silico test is not specific for fungal membranes, which have physicochemical characteristics different from those of mammalian cells, such as lipid composition and electrostatic charge. The second hypothesis is that permeabilization is a secondary consequence of oxidative stress. Recent studies have suggested that other intracellular targets of AMPs and the capacity for membrane permeabilization could be secondary events caused by the endogenous increase in ROS production [80–82]. AMPs tend to exhibit selective toxicity because of their biochemical characteristics, and are considered promising sources of new molecules with therapeutic potential [16]. Nevertheless, it is important to evaluate the toxicity of any AMP-derived drug candidate in mammalian cells for approval by regulatory agencies. Hemolytic activity is a test system used in quantitative cytotoxicity assays. We observed that *Ca*CDef-like were not toxic to sheep erythrocytes at all the concentrations tested ($CC_{50} > 400$ μg L^{-1}) and that *Ca*CLTP2 had low toxicity at the concentrations used in antifungal tests (200 μg L^{-1}). Thus, the effects of these peptides on yeast cells did not match their cytotoxicity toward erythrocytes, thereby showing selectivity.

In conclusion, our study demonstrated that three novel AMPs isolated from *C. annuum* leaves. These AMPs displayed in vitro antifungal activity against some pathogenic *Candida* species, and *Ca*CPin-II was toxic to mammalian cells under the tested conditions. Thus, we suggest that *Ca*CPin-II, *Ca*CDef-like, and *Ca*CLTP2 are promising peptides for the development of novel antifungal treatments.

Supplementary Information The online version contains supplementary material available at https://doi.org/10.1007/s12602-023-10112-3.

Acknowledgements This work was performed at the Universidade Estadual do Norte Fluminense Darcy Ribeiro (UENF). We wish to thank L.C.D. Souza and V.M. Kokis for technical assistance.

Author Contribution The study was conceived by MBC and VMG. Experimental procedures were carried out by MBC, GBT, F A-S, MSS, MCC, ATSF, and RR. Data analyses were performed by MBC, JAAP, TMV, AOC, RR, OVM, and MARBC. The paper was written by MBC, GBT, FA-S, and VMG. All authors reviewed the manuscript.

Funding We acknowledge the financial support of the Brazilian agencies CNPq (307590/2021–6), FAPERJ (E-26/200567/2023; E-26/210353/2022). This study was also financed in part by the Coordenação de Aperfeiçoamento de Pessoal de Nível Superior – Brazil (CAPES), finance code 001.

Data Availability All data generated or analyzed during this study are included in this published article.

Declarations

Ethics Approval This article does not contain any studies with human or animal subjects.

Conflict of Interest The authors declare no conflict of interest.

References

1. Mookherjee N, Anderson MA, Haagsman HP, Davidson DJ (2020) Antimicrobial host defence peptides: functions and clinical potential. Nat Rev Drug Discov 19:311–332. https://doi.org/10.1038/s41573-019-0058-8
2. Huan Y, Kong Q, Mou H, Yi H (2020) Antimicrobial peptides: classification, design, application and research progress in multiple fields. Front Microbiol 11:1–21. https://doi.org/10.3389/fmicb.2020.582779
3. Ojeda PG, Cardoso MH, Franco OL (2019) Pharmaceutical applications of cyclotides. Drug Discov Today 24:2152–2161. https://doi.org/10.1016/j.drudis.2019.09.010
4. Zasloff M (2019) Antimicrobial peptides of multicellular organisms: my perspective. Adv Exp Med Biol 1117:3–6. https://doi.org/10.1007/978-981-13-3588-4_1
5. Padovan L, Scocchi M, Tossi A (2010) Structural aspects of plant antimicrobial peptides. Curr Protein Pept Sci 11:210–219. https://doi.org/10.2174/138920310791112093
6. Campos ML, Lião LM, Alves ES et al (2018) A structural perspective of plant antimicrobial peptides. Biochem J 475:3359–3375. https://doi.org/10.1042/BCJ20180213
7. Ahmed TAE, Hammami R (2019) Recent insights into structure–function relationships of antimicrobial peptides. J Food Biochem 43:1–8. https://doi.org/10.1111/jfbc.12546
8. Campos ML, De Souza CM, De Oliveira KBS et al (2018) The role of antimicrobial peptides in plant immunity. J Exp Bot 69:4997–5011. https://doi.org/10.1093/jxb/ery294
9. Fisher MC, Henk DA, Briggs CJ et al (2012) Emerging fungal threats to animal, plant and ecosystem health. Nature 484:186–194. https://doi.org/10.1038/nature10947
10. GAFFI (2020) Global action fund for fungal infection. https://www.gaffi.org/. Accessed 29 May 2020
11. Giacomazzi J, Baethgen L, Carneiro LC et al (2016) The burden of serious human fungal infections in Brazil. Mycoses 59:145–150. https://doi.org/10.1111/myc.12427
12. CDC (2019) Antibiotic resistance threats in the United States. Atlanta, GA: U.S Department of Health and Human Services. https://www.cdc.gov/DrugResistance/. Accessed 20 Dec 2022
13. CDC (2013) *Candida auris*: a drug-resistant germ that spreads in healthcare facilities. Centers for Disease Control and Prevention. https://www.cdc.gov/fungal/diseases/candidiasis/pdf/Candida_auris_508.pdf. Accessed 20 Dec 2022
14. Koo HB, Seo J (2019) Antimicrobial peptides under clinical investigation. Pept Sci. https://doi.org/10.1002/pep2.24122
15. Lewies A, Du Plessis LH, Wentzel JF (2019) Antimicrobial peptides: the Achilles' heel of antibiotic resistance? Probiotics Antimicrob Proteins 11:370–381. https://doi.org/10.1007/s12602-018-9465-0
16. Divyashree M, Mani MK, Reddy D et al (2019) Clinical applications of antimicrobial peptides (AMPs): where do we stand now? Protein Pept Lett 27:120–134. https://doi.org/10.2174/0929866526666190925152957
17. Lei J, Sun LC, Huang S et al (2019) The antimicrobial peptides and their potential clinical applications. Am J Transl Res 11:3919–3931
18. Afroz M, Akter S, Ahmed A et al (2020) Ethnobotany and antimicrobial peptides from plants of the Solanaceae family: an update and future prospects. Front Pharmacol. https://doi.org/10.3389/fphar.2020.00565
19. da Silva Gebara R, Taveira GB, de Azevedo dos Santos L et al (2020) Identification and characterization of two defensins from *Capsicum annuum* fruits that exhibit antimicrobial activity. Probiotics Antimicrob Proteins 12:1253–1265. https://doi.org/10.1007/s12602-020-09647-6
20. Maracahipes ÁC, Taveira GB, Mello EO et al (2019) Biochemical analysis of antimicrobial peptides in two different *Capsicum* genotypes after fruit infection by *Colletotrichum gloeosporioides*. Biosci Rep 39:BSR20181889. https://doi.org/10.1042/BSR20181889
21. Anaya-López JL, López-Meza JE, Baizabal-Aguirre VM et al (2006) Fungicidal and cytotoxic activity of a *Capsicum chinense* defensin expressed by endothelial cells. Biotechnol Lett 28:1101–1108. https://doi.org/10.1007/s10529-006-9060-4
22. Diz MSS, Carvalho AO, Rodrigues R et al (2006) Antimicrobial peptides from chilli pepper seeds causes yeast plasma membrane permeabilization and inhibits the acidification of the medium by yeast cells. Biochim Biophys Acta - Gen Subj 1760:1323–1332. https://doi.org/10.1016/j.bbagen.2006.04.010
23. da Silva Pereira L, do Nascimento VV, de Fátima Ferreira Ribeiro S et al (2018) Characterization of *Capsicum annuum* L. leaf and root antimicrobial peptides: antimicrobial activity against phytopathogenic microorganisms. Acta Physiol Plant 40:1–15. https://doi.org/10.1007/s11738-018-2685-9
24. Ribeiro SFF, Carvalho AO, Da Cunha M et al (2007) Isolation and characterization of novel peptides from chilli pepper seeds: antimicrobial activities against pathogenic yeasts. Toxicon 50:600–611. https://doi.org/10.1016/j.toxicon.2007.05.005
25. Taveira GB, Da Motta OV, Machado OLT et al (2014) Thionin-like peptides from *Capsicum annuum* fruits with high activity against human pathogenic bacteria and yeasts. Biopolym - Pept Sci Sect 102:30–39. https://doi.org/10.1002/bip.22351
26. Díaz-Murillo V, Medina-Estrada I, López-Meza JE, Ochoa-Zarzosa A (2016) Defensin γ-thionin from *Capsicum chinense* has immunomodulatory effects on bovine mammary epithelial cells during *Staphylococcus aureus* internalization. Peptides 78:109–118. https://doi.org/10.1016/j.peptides.2016.02.008
27. Games PD, Da Silva EQG, Barbosa MDO et al (2016) Computer aided identification of a Hevein-like antimicrobial peptide of bell pepper leaves for biotechnological use. BMC Genomics 17:1–13. https://doi.org/10.1186/s12864-016-3332-8
28. Taveira GB, Mello ÉO, Souza SB et al (2018) Programmed cell death in yeast by thionin-like peptide from *Capsicum annuum* fruits involving activation of caspases and extracellular H^+ flux. Biosci Rep 38:1–27. https://doi.org/10.1042/BSR20180119

29. Silva MS, Ribeiro SFF, Taveira GB et al (2017) Application and bioactive properties of CaTI, a trypsin inhibitor from *Capsicum annuum* seeds: membrane permeabilization, oxidative stress and intracellular target in phytopathogenic fungi cells. J Sci Food Agric 97:3790–3801. https://doi.org/10.1002/jsfa.8243
30. Smith PK, Krohn RI, Hermanson GT et al (1985) Measurement of protein using bicinchoninic acid. Anal Biochem 150:76–85. https://doi.org/10.1016/0003-2697(85)90442-7
31. Schägger H, von Jagow G (1987) Tricine-sodium dodecyl sulfate-polyacrylamide gel electrophoresis for the separation of proteins in the range from 1 to 100 kDa. Anal Biochem 166:368–379. https://doi.org/10.1016/0003-2697(87)90587-2
32. Altschul SF, Gish W, Miller W et al (1990) Basic local alignment search tool. J Mol Biol 215:403–410
33. Yadav NK, Saikhedkar NS, Giri AP (2021) PINIR: a comprehensive information resource for Pin-II type protease inhibitors. BMC Plant Biol 21
34. Thompson JD, Higgins DG, Gibson TJ (1994) CLUSTAL W: improving the sensitivity of progressive multiple sequence alignment through sequence weighting, position-specific gap penalties and weight matrix choice. Nucleic Acids Res 22:4673–4680. https://doi.org/10.1093/nar/22.22.4673
35. Jumper J, Evans R, Pritzel A et al (2021) Highly accurate protein structure prediction with AlphaFold. Nature 596:583–589. https://doi.org/10.1038/s41586-021-03819-2
36. Kelley LA, Mezulis S, Yates CM et al (2016) The Phyre2 web portal for protein modeling, prediction and analysis. Nat Protoc 10:845–858. https://doi.org/10.1038/nprot.2015-053
37. Wei L, Tang J, Zou Q (2017) SkipCPP-Pred: an improved and promising sequence-based predictor for predicting cell-penetrating peptides. BMC Genomics 18:1–11. https://doi.org/10.1186/s12864-017-4128-1
38. Manavalan B, Subramaniyam S, Shin TH et al (2018) Machine-learning-based prediction of cell-penetrating peptides and their uptake efficiency with improved accuracy
39. Kumar V, Agrawal P, Kumar R et al (2018) Prediction of cell-penetrating potential of modified peptides containing natural and chemically modified residues. Front Microbiol 9:1–10. https://doi.org/10.3389/fmicb.2018.00725
40. Agrawal P, Bhalla S, Usmani SS et al (2016) CPPsite 2.0: a repository of experimentally validated cell-penetrating peptides. Nucleic Acids Res 44:D1098–D1103. https://doi.org/10.1093/nar/gkv1266
41. de Oliveira Mello É, Taveira GB, de Oliveira Carvalho A, Gomes VM (2019) Improved smallest peptides based on positive charge increase of the γ-core motif from PνD 1 and their mechanism of action against *Candida* species. Int J Nanomedicine 14:407–420. https://doi.org/10.2147/IJN.S187957
42. Broekaert WF, Terras FRG, Cammue BPA, Vanderleyden J (1990) An automated quantitative assay for fungal growth inhibition. FEMS Microbiol Lett 69:55–59. https://doi.org/10.1016/0378-1097(90)90412-J
43. Deere D, Shen J, Vesey G et al (1998) Flow cytometry and cell sorting for yeast viability assessment and cell selection. Yeast 14:147–160. https://doi.org/10.1002/(SICI)1097-0061(19980130)14:2%3c147::AID-YEA207%3e3.0.CO;2-L
44. Thevissen K, Terras FRG, Broekaert WF (1999) Permeabilization of fungal membranes by plant defensins inhibits fungal growth. Appl Environ Microbiol 65:5451–5458. https://doi.org/10.1128/aem.65.12.5451-5458.1999
45. Labno C (2014) Two ways to count cells with ImageJ. Integr Light Microsc Core. https://www.unige.ch/medecine/bioimaging/files/3714/1208/5964/CellCounting.pdf. Accessed 20 Dec 2022
46. Mello EO, Ribeiro SFF, Carvalho AO et al (2011) Antifungal activity of PvD1 defensin involves plasma membrane permeabilization, inhibition of medium acidification, and induction of ROS in fungi cells. Curr Microbiol 62:1209–1217. https://doi.org/10.1007/s00284-010-9847-3
47. Bernfeld P (1955) Amylases, alpha and beta. Methods Enzymol I I:149–158. https://doi.org/10.1016/0076-6879(55)01021-5
48. Macedo MLR, Garcia VA, Maria das Graças MF, Richardson M (2007) Characterization of a Kunitz trypsin inhibitor with a single disulfide bridge from seeds of *Inga laurina* (SW.) Willd. Phytochemistry 68:1104–1111. https://doi.org/10.1016/j.phytochem.2007.01.024
49. Michaud D, Nguyen-Quoc B, Bernier-Vadnais N et al (1994) Cysteine proteinase forms in sprouting potato tuber. Physiol Plant 90:497–503. https://doi.org/10.1111/j.1399-3054.1994.tb08807.x
50. Oren Z, Shai Y (1997) Selective lysis of bacteria but not mammalian cells by diastereomers of melittin: structure-function study. Biochemistry 36:1826–1835. https://doi.org/10.1021/bi962507l
51. Li J, Hu S, Jian W et al (2021) Plant antimicrobial peptides: structures, functions, and applications. Bot Stud 62:1–15
52. dos Santos-Silva CA, Zupin L, Oliveira-Lima M et al (2020) Plant antimicrobial peptides: state of the art, in silico prediction and perspectives in the omics era. Bioinform Biol Insights. https://doi.org/10.1177/1177932220952739
53. Diz MS, Carvalho AO, Ribeiro SFF et al (2011) Characterisation, immunolocalisation and antifungal activity of a lipid transfer protein from chili pepper (*Capsicum annuum*) seeds with novel α-amylase inhibitory properties. Physiol Plant 142:233–246. https://doi.org/10.1111/j.1399-3054.2011.01464.x
54. Yeon ML, Hyoung SW, Ahn IP et al (2004) Molecular characterization of a cDNA for a cysteine-rich antifungal protein from *Capsicum annuum*. J Plant Biol 47:375–382. https://doi.org/10.1007/bf03030554
55. CDC (2020) CDC and fungal diseases: why are fungal diseases a public health issue? Centers for Disease Control and Prevention. https://www.cdc.gov/fungal/. Accessed 20 Dec 2022
56. Gartia J, Anangi R, Joshi RS et al (2020) NMR structure and dynamics of inhibitory repeat domain variant 12, a plant protease inhibitor from *Capsicum annuum*, and its structural relationship to other plant protease inhibitors. J Biomol Struct Dyn 38:1388–1397
57. Tamhane VA, Mishra M, Mahajan NS et al (2012) Plant Pin-II family proteinase Inhibitors : structural and functional diversity. Funct Plant Sci Biotecnol 6:42–58
58. Bártová V, Bárta J, Jarošová M (2019) Antifungal and antimicrobial proteins and peptides of potato (*Solanum tuberosum* L.) tubers and their applications. Appl Microbiol Biotechnol 103:5533–5547. https://doi.org/10.1007/s00253-019-09887-9
59. Kim JY, Park SC, Kim MH et al (2005) Antimicrobial activity studies on a trypsin-chymotrypsin protease inhibitor obtained from potato. Biochem Biophys Res Commun 330:921–927. https://doi.org/10.1016/j.bbrc.2005.03.057
60. Barrette-Ng IH, Ng KKS, Cherney MM et al (2003) Unbound form of tomato inhibitor-II reveals interdomain flexibility and conformational variability in the reactive site loops. J Biol Chem 278:31391–31400
61. Schirra HJ, Guarino RF, Anderson MA, Craik DJ (2010) Selective removal of individual disulfide bonds within a potato type II serine proteinase inhibitor from *Nicotiana alata* reveals differential stabilization of the reactive-site loop. J Mol Biol 395:609–626
62. Barrette-Ng IH, Ng KKS, Cherney MM et al (2003) Structural basis of inhibition revealed by a 1:2 complex of the two-headed tomato inhibitor-II and subtilisin Carlsberg. J Biol Chem 278:24062–24071
63. Mishra M, Tamhane VA, Khandelwal N et al (2010) Interaction of recombinant CanPIs with *Helicoverpa armigera* gut proteases reveals their processing patterns, stability and efficiency. Proteomics 10:2845–2857. https://doi.org/10.1002/pmic.200900853
64. Parisi K, Shafee TMA, Quimbar P et al (2019) The evolution, function and mechanisms of action for plant defensins. Semin Cell Dev Biol 88:107–118. https://doi.org/10.1016/j.semcdb.2018.02.004

65. Viega de Andrade EK, Rodrigues R, da Costa Vieira Bard G et al (2020) Identification, biochemical characterization and biological role of defense proteins from common bean genotypes seeds in response to *Callosobruchus maculatus* infestation. J Stored Prod Res. https://doi.org/10.1016/j.jspr.2020.101580
66. Yount NY, Yeaman MR (2004) Multidimensional signatures in antimicrobial peptides. Proc Natl Acad Sci U S A 101:7363–7368. https://doi.org/10.1073/pnas.0401567101
67. de Oliveira CA, Moreira Gomes V (2012) Plant defensins and defensin-like peptides—biological activities and biotechnological applications. Curr Pharm Des 17:4270–4293. https://doi.org/10.2174/138161211798999447
68. Sher Khan R, Iqbal A, Malak R et al (2019) Plant defensins: types, mechanism of action and prospects of genetic engineering for enhanced disease resistance in plants. 3 Biotech 9:1–12. https://doi.org/10.1007/s13205-019-1725-5
69. Edqvist J, Blomqvist K, Nieuwland J, Salminen TA (2018) Plant lipid transfer proteins: are we finally closing in on the roles of these enigmatic proteins? J Lipid Res 59:1374–1382. https://doi.org/10.1194/jlr.R083139
70. Melnikova DN, Finkina EI, Bogdanov IV et al (2023) Features and possible applications of plant lipid-binding and transfer proteins. Membranes 13:1–17
71. Edstam MM, Viitanen L, Salminen TA, Edqvist J (2011) Evolutionary history of the non-specific lipid transfer proteins. Mol Plant 4:947–964. https://doi.org/10.1093/mp/ssr019
72. Missaoui K, Gonzalez-Klein Z, Pazos-Castro D et al (2022) Plant non-specific lipid transfer proteins: an overview. Plant Physiol Biochem 171:115–127. https://doi.org/10.1016/j.plaphy.2021.12.026
73. Cruz LP, Ribeiro SFF, Carvalho AO et al (2010) Isolation and partial characterization of a novel lipid transfer protein (LTP) and antifungal activity of peptides from chilli pepper seeds. Protein Pept Lett 17:311–318
74. Carvalho AO, Souza-Filho GA, Ferreira BS et al (2006) Cloning and characterization of a cowpea seed lipid transfer protein cDNA: expression analysis during seed development and under fungal and cold stresses in seedlings' tissues. Plant Physiol Biochem 44:732–742. https://doi.org/10.1016/j.plaphy.2006.09.011
75. Bard GCV, Taveira GB, Souza TAM et al (2018) *Coffea canephora* peptides in combinatorial treatment with fluconazole: antimicrobial activity against phytopathogenic fungus. Int J Microbiol. https://doi.org/10.1155/2018/8546470
76. Zottich U, Da M, Carvalho AO et al (2011) Purification, biochemical characterization and antifungal activity of a new lipid transfer protein (LTP) from *Coffea canephora* seeds with α -amylase inhibitor properties. BBA - Gen Subj 1810:375–383. https://doi.org/10.1016/j.bbagen.2010.12.002
77. Salminen TA, Blomqvist K, Edqvist J (2016) Lipid transfer proteins: classification, nomenclature, structure, and function. Planta 244:971–997
78. Dias GB, Gomes VM, Pereira UZ et al (2013) Isolation, characterization and antifungal activity of proteinase inhibitors from *Capsicum chinense* Jacq. seeds. Protein J 32:15–26. https://doi.org/10.1007/s10930-012-9456-z
79. Davey HM, Hexley P (2011) Red but not dead? Membranes of stressed *Saccharomyces cerevisiae* are permeable to propidium iodide. Environ Microbiol 13:163–171. https://doi.org/10.1111/j.1462-2920.2010.02317.x
80. Shackelford RE, Kaufmann WK, Paules RS (2000) Oxidative stress and cell cycle checkpoint function. Free Radic Biol Med 28:1387–1404. https://doi.org/10.1016/S0891-5849(00)00224-0
81. Soares JR, Tenório J, de Melo E, da Cunha M et al (2017) Interaction between the plant ApDef1 defensin and *Saccharomyces cerevisiae* results in yeast death through a cell cycle- and caspase-dependent process occurring via uncontrolled oxidative stress. Biochim Biophys Acta - Gen Subj 1861:3429–3443. https://doi.org/10.1016/j.bbagen.2016.09.005
82. Yeaman MR, Büttner S, Thevissen K (2018) Regulated cell death as a therapeutic target for novel antifungal peptides and biologics. Oxid Med Cell Longev. https://doi.org/10.1155/2018/5473817
83. Sun JY, Gaudet DA, Lu ZX et al (2008) Characterization and antifungal properties of wheat nonspecific lipid transfer proteins. Mol Plant-Microbe Interact 21:346–360. https://doi.org/10.1094/MPMI-21-3-0346
84. Ge X, Chen J, Li N et al (2003) Resistance function of rice lipid transfer protein LTP110. J Biochem Mol Biol 36:603–607
85. Finkina EI, Melnikova DN, Bogdanov IV, Ovchinnikova TV (2016) Lipid transfer proteins as components of the plant innate immune system: structure, functions, and applications. Acta Naturae 8:47–61. https://doi.org/10.32607/20758251-2016-8-2-47-61
86. Kulkarni MM, Mcmaster WR, Kamysz W, Mcgwire BS (2009) Antimicrobial peptide-induced apoptotic death of *Leishmania* results from calcium-dependent, caspase-independent mitochondrial toxicity *. J Biol Chem 284:15496–15504. https://doi.org/10.1074/jbc.M809079200
87. Aerts AM, François IEJA, Meert EMK et al (2007) The antifungal activity of RsAFP2, a plant defensin from *Raphanus sativus*, involves the induction of reactive oxygen species in *Candida albicans*. J Mol Microbiol Biotechnol 13:243–247. https://doi.org/10.1159/000104753
88. Kowaltowski AJ, de Souza-Pinto NC, Castilho RF, Vercesi AE (2009) Mitochondria and reactive oxygen species. Free Radic Biol Med 47:333–343. https://doi.org/10.1016/j.freeradbiomed.2009.05.004
89. Rudzińska M, Daglioglu C, Savvateeva LV et al (2021) Current status and perspectives of protease inhibitors and their combination with nanosized drug delivery systems for targeted cancer therapy. Drug Des Devel Ther 15:9–20. https://doi.org/10.2147/DDDT.S285852
90. Gutierrez-Gongora D, Geddes-Mcalister J (2021) From naturally-sourced protease inhibitors to new treatments for fungal infections. J Fungi. https://doi.org/10.3390/jof7121016
91. Dib HX, de Oliveira DGL, de Oliveira CFR et al (2019) Biochemical characterization of a Kunitz inhibitor from *Inga edulis* seeds with antifungal activity against Candida spp. Arch Microbiol 201:223–233. https://doi.org/10.1007/s00203-018-1598-8
92. Macedo MLR, Ribeiro SFF, Taveira GB et al (2016) Antimicrobial activity of ILTI, a Kunitz-type trypsin inhibitor from *Inga laurina* (SW.) Willd. Curr Microbiol 72:538–544. https://doi.org/10.1007/s00284-015-0970-z
93. Pimenta S, Rodrigues R, Sudré CP et al (2016) Protecting vegetable cultivars in Brazil: a chili pepper case-study research. Hortic Bras 34:161–167
94. Franco OL, Rigden DJ, Melo FR, Grossi-de-Sá MF (2002) Plant α-amylase inhibitors and their interaction with insect α-amylases: structure, function and potential for crop protection. Eur J Biochem 269:397–412. https://doi.org/10.1046/j.0014-2956.2001.02656.x
95. Grosse-Holz FM, van der Hoorn RAL (2016) Juggling jobs: roles and mechanisms of multifunctional protease inhibitors in plants. New Phytol 210:794–807. https://doi.org/10.1111/nph.13839